J. Plasma Fusion Res. SERIES, Vol. 3 (2000) 431–435

The Study on the Neoclassical Transport Analysis using ECE Measured Temperature Profiles in the LHD Long Pulse Plasma

SASAO Hajime*, WATANABE Kiyomasa[1], INAGAKI Shigeru[1], NAGAYAMA Yoshio[1], PETER. C. de Vries[1], TANAKA Kenji[1], TOKUZAWA Tokihiko[1], KAWAHATA Kazuo[1], NARIHARA Kazuto[1], YAMADA Ichihiro[1], IDA Katsumi[1], KADO Shinichirou[1], KUBO Shin[1], KOMORI Akio[1], YAMADA Hiroshi[1], KANEKO Osamu[1], MOTOJIMA Osamu[1] and LHD Exp. Group 1 and 2

Department of Fusion Science, The Graduate University for Advanced Studies, Toki-shi, Japan

[1]National Institute for Fusion Science, 322-6 Oroshi-cho, Toki-shi, 509-5292, Japan

(Received: 18 January 2000 / Accepted: 19 April 2000)

Abstract

The purpose of this paper is to show the change of the neoclassical transport and the radial electric field in the long pulse LHD plasmas by using the experimental ECE data. The neoclassical heat flux, which the neo-classical theory predicts, changes due to the change of the radial electric field. The increase of H ions injected by Neutral Beam Injection (NBI) in He discharge produce effect on the electric field. There is the threshold of H quantity on the change of the electric field polarity.

Keywords:

ECE, neoclassical transport theory, radial electric field

1. Introduction

In long pulse NBI helium discharge, the density of hydrogen increases with the extension of the discharge time. For example, in the case of 10 keV and 1 MW NBI discharge, the quantity of the injected H is about 2 $\times 10^{18}$ m^{-2} s^{-1} in 30 m^{-3} devices. In He plasmas, it is possible that this increment of H affects the transport of ions and electrons, which leads to the change of radial electric field polarity according to the ambipolar condition. In this paper, we apply the ECE data to study the change of the neoclassical transport and the radial electric field in the long pulse LHD plasmas.

2. The ECE Diagnostics

The LHD has two electron cyclotron resonance regions in the equatorial plane because magnetic field strength does not change monotonically when traversing the plasma from the inboard to outboard sides. The electron cyclotron wave, which is emitted from the torus inner electron cyclotron resonance region, is absorbed in the outboard resonance region. Therefore, it is difficult to measure the electron temperature of the torus region from the outside ports with the ECE diagnostics. We installed an antenna at the inner torus port of the LHD in order to measure the emission of the electron cyclotron wave that propagates to the center of torus. The ECE inner antenna is designed with gaussian beam optics and is based on the concept of the constant phase, proposed by S. Kubo *et al.* [1]. This concept indicates that the surface of the antenna is decided by the following condition; the sum of the microwave phases calculated from two points, which are the start point and the end point of the wave trace, is constant on the

Corresponding author's e-mail: hsasao@ms.nifs.ac.jp

antenna surface.

In this study, the electron temperature profile is measured with a 32ch-heterodyne radiometer. It covers the fundamental harmonic of O-mode emission in the frequency range of 64–86 GHz in the case of $B_0 = 2.75$ T operation [2]. The ECE electron temperature is calibrated with the data obtained by the Thomson scattering measurement.

3. Neoclassical Transport and the Radial Electric Field

The neoclassical radial electric field in the heliotron/torsatron plasmas is decided by the ambipolar condition:

$$\sum_a Z_a \Gamma_a^{na} = 0 , \tag{1}$$

where Z_a, Γ_a^{na} are the atomic number and the radial particle flux of species a in the non-axisymetric magnetic configuration. Shaing *et al.* gave the formula of the particle flux Γ_a^{na} and the heat flux Q_a^{na} [3].

$$\Gamma_a = -\varepsilon_t^2 \varepsilon_h^{1/2} \nu_{da}^2 n_a \int_0^\infty dx\, x^{5/2} e^{-x} \tilde{\nu}_a(x) \frac{A_a(x, E_r)}{\omega_a^2(x, E_r)} , \tag{2}$$

$$Q_a = -\varepsilon_t^2 \varepsilon_h^{1/2} \nu_{da}^2 n_a T_a \int_0^\infty dx\, x^{5/2} e^{-x} \tilde{\nu}_a(x) \frac{A_a(x, E_r)}{\omega_a^2(x, E_r)} , \tag{3}$$

where,

$$A_a(x, E_r) \equiv \frac{dn_a/dt}{n_a} - \frac{Z_a e E_r}{T_a} + (x - \frac{3}{2}) \frac{dT_a/dt}{n_a} ,$$

$$x \equiv \frac{1}{2} m_a v^2 / T_a , \quad \tilde{\nu}_a \equiv \nu_{tha} / (\varepsilon_h x^{3/2}) ,$$

$$\nu_{da} \equiv -T_a / (Z_a erB) , \quad \omega_a^2 = \omega_{1/\nu}^2 + \omega_p^2 + \omega_{sb}^2 + \omega_\nu^2$$

Here $\omega_{1/\nu}$, ω_p, ω_{sb} and ω_ν are the angular frequency in the region of the $1/\nu$ collisional regime, the helical ripple plateau regime, the resonant superbanana, and collisionless detrapping regime respectively. ν_{tha}, ν are thermal velocity and the collisionality. T_a, m_a, n_a, ε_t, ε_h and B are the temperature, the mass and density of species a, the toroidal ripple, helical ripple and the magnetic field.

In our study, He, H and electron are considered as plasma species. Then, the ambipolar condition is written as,

$$Z_e \Gamma_e^{na} + Z_{He} \Gamma_{He}^{na} + Z_H \Gamma_H^{na} = 0 . \tag{4}$$

In order to estimate the electric field E_r, we solve eq. (4) with the experimental data; the electron temperature T_e, the ion temperature T_i and the electron density n_e. The electron and ion neoclassical thermal conductivity $X_{i\_non\text{-}ax}$, $X_{e\_non\text{-}ax}$, in non-aximmetric magnetic configuration are given by,

$$X_{i\_non\text{-}ax} = -Q_i^{na} / n_i \nabla T_i , \tag{5}$$

$$X_{e\_non\text{-}ax} = -Q_e^{na} / n_e \nabla T_e . \tag{6}$$

4. The Experimental Results

4.1 Neoclassical transport in long pulse plasmas

In order to study the behavior of the neoclassical transport, we analyze a typical example og a long pulse discharge. The discharge starts by ECH and it has been sustained by NBI for 35 s on 2.75 T operation.

Figure 1 shows the time evolution of W_p, T_e, T_i, n_e. T_e is measured with a ECE system. T_i is measured with a charge exchange spectrscopy [4], and n_e is measured with a far-infrared laser interferometer [5]. The electron density profiles are constructed by Abel inversion method. W_p is estimated by the Diamagnetic flux measurement. ECH is supplied for first 1 s. Two NB are injected, but one NB injection is terminated at $t = 5$ s. The He gas is puffed until $t = 17$ s. T_e and T_i remain at a high level, and then they decrease after $t = 5$ s.

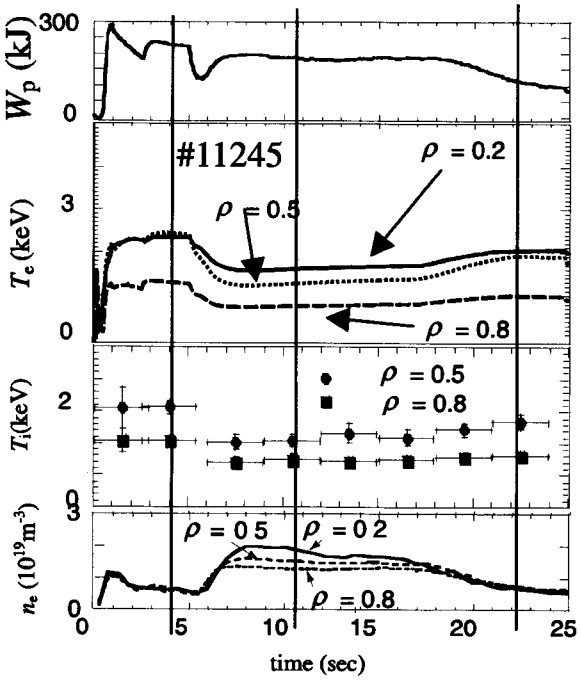

Fig. 1 The time evolution of W_p, T_e, T_i and n_e. Three solid lines indicate the time evolution of W_p, T_e and n_e at $\rho = 0.2$.

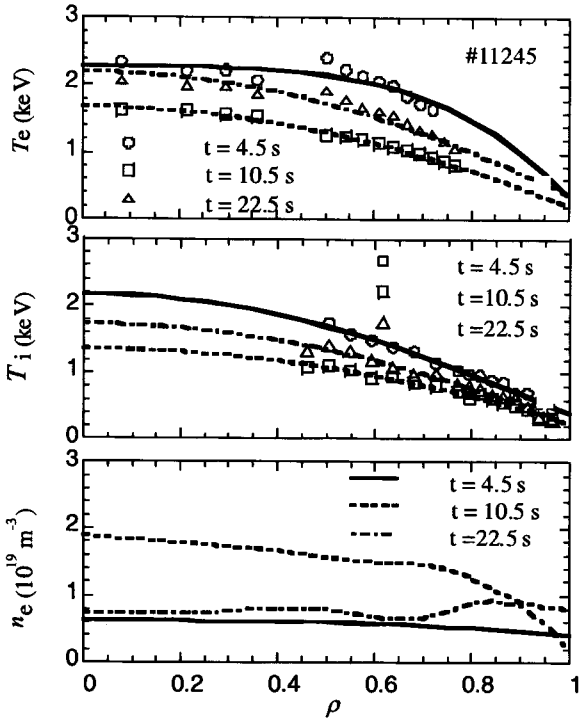

Fig. 2 The profiles of T_e, T_i and n_e at t = 4.5 s, t = 10.5 s and t = 22.5 s.

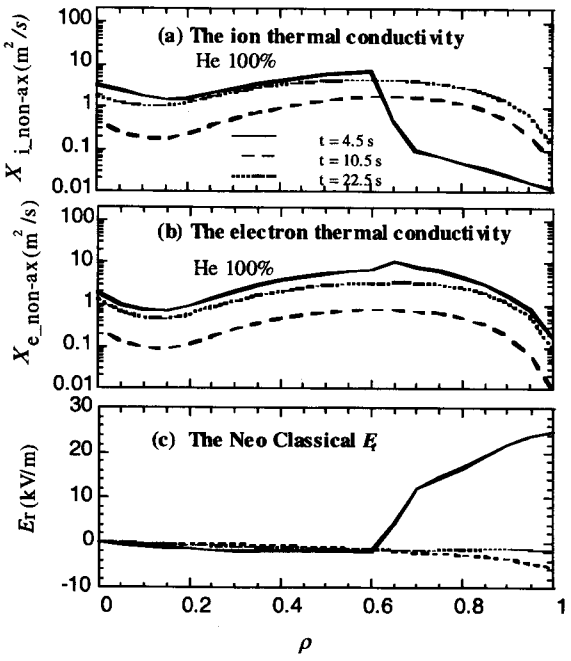

Fig. 3 (a) the ion thermal conductivity, (b) the electron thermal conductivity and (c) the radial electric field.

Afterward, they increase gradually. On the other hand, n_e is constant before t = 5 s and it increases until t = 8 s, then it decreases. We analyze the radial electric field of this discharge at t = 4.5 s when T_e starts to decrease (case (1)), at t = 10.5 s when T_e and n_e are constant (case (2)), and at 22.5 s when n_e is decreasing (case (3)). The profiles of T_e, T_i and n_e are shown in Fig. 2. The lines in Fig. 2 are the fitting curves. We apply the fitting data to the caluculation of the electric field and the thermal conductivity.

The neoclassical thermal conductivity profile of non-axisymetric plasmas and electric field profile are shown in Fig. 3. $X_{i\_non\text{-}ax}$, $X_{e\_non\text{-}ax}$ and E_r are estimated with experimental data of T_e, T_i and n_e. We can find in Fig. 3 (a) that $X_{i\_non\text{-}ax}$ becomes small in the periphery of plasma at t = 4.5 s though the decrement of $X_{i\_non\text{-}ax}$ is not found at t = 10.5 s and at t = 22.5 s. On the other hand, the decrease in $X_{e\_non\text{-}ax}$ at the periphery doesn't appear in Fig. 3 (b). The reason is the following. At t = 4.5 s, the large positive electric field is predicted and the plasma is in the electron root as shown in Fig. 3 (c).

In Figs. 4, the time evolution of $X_{i\_non\text{-}ax}$, $X_{e\_non\text{-}ax}$ and E_r at ρ = 0.8 is shown. Here, we interpolated T_i data linearly between measurement points of T_i time series

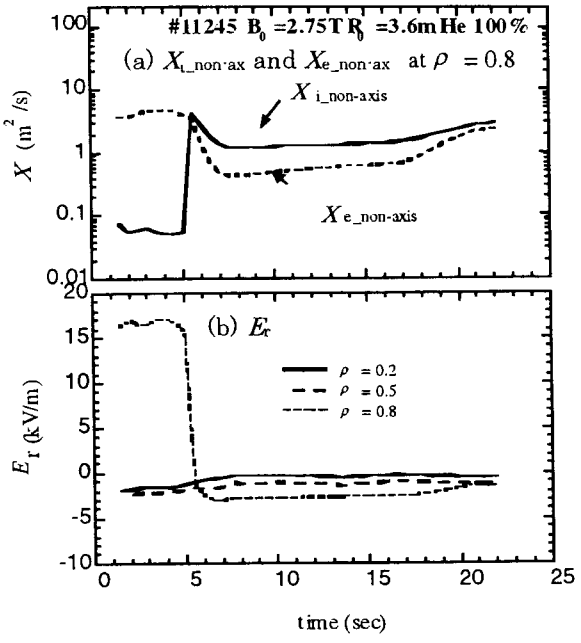

Fig. 4 (a) The time evolution o $X_{i\_non\text{-}ax}$, $X_{e\_non\text{-}ax}$ and (b) E_r.

and take an average of T_e and n_e for 3.0 sec which corresponds to the accumulation time of T_i

measurement. The conductivity of ions is quite smaller than that of electrons before t = 5 s. Afterward, $X_{i\_non\text{-}ax}$ increases, then both of $X_{i\_non\text{-}ax}$ and $X_{e\_non\text{-}ax}$ decrease and they hold the constant value. Figure 4 (b) shows the time evolution of E_r at ρ = 0.8. The positive E_r changes to be negative at t = 5 s. Until t = 5 s, the electron root plasmas is predicted and $X_{i\_non\text{-}ax}$ has a small value in the periphery. And $X_{e\_non\text{-}ax}$ after t = 5 s becomes smaller than the value before t = 5 s because of the small negative electric field which corresponds to the ion root plasma.

4.2 The effect of the H injection

We study the effects of the H injection on $X_{i\_non\text{-}ax}$ and $X_{e\_non\text{-}ax}$ at t = 4.5 s. Figures 5 show the profile of $X_{i\_non\text{-}ax}$ and $X_{e\_non\text{-}ax}$ for different ratios of He and H. We find that $X_{i\_non\text{-}ax}$ becomes large when the ratio of H increases. On the contrary, a large difference is not found about $X_{e\_non\text{-}ax}$. The dependence of the atomic number Z and atomic mass number A on the flux of ions in the $1/v$ region is written as,

$$Z_i\Gamma_i = -Z_i D\frac{\partial n_i}{\partial r} \propto Z_i(Z_i^{-2}\nu_{ii}^{-1})Z_i^{-1}\frac{\partial n_e}{\partial r}, \quad \propto Z_i^{-5}A_i^{1/2}, \tag{7}$$

where ν_{ii} is collision frequency between ions. When on the contraty, the flux of electrons is written as,

$$\Gamma_e = -D\frac{\partial n_e}{\partial r} \propto (\nu_{ei}^{-1})\frac{\partial n_e}{\partial r} \propto Z_{eff}^{-1}, \tag{8}$$

where Z_{eff} is the effective charge. The ratio of ion and electron flux is written as,

$$\Pi_e \equiv Z_i\Gamma_i/\Gamma_e \propto Z_i^{-5}A^{1/2}Z_{eff}. \tag{9}$$

In the case of H and He, the ratio is, Π_H/Π_{He} ~ 16. Here, we assume Z_{eff} is same between H plasmas and He plasmas. It is expected that the diffusion of ions becomes large when H is injected, the negative E_r is generated and as a result, the ion conductivity becomes large. In fig. 6, the profile of E_r is shown when the different ratio of He and H at t = 4.5 s is assumed. When the ratio of H increases, the positive E_r turns to be negative in the periphery. The sign of E_r suddenly changes when the ratio increases from 30% to 40 % as shown in Fig. 6.

5. Summary

In order to study the behavior of the neoclassical thermal conductivity and the radial electric field, we applied the ECE experimental data with the inner

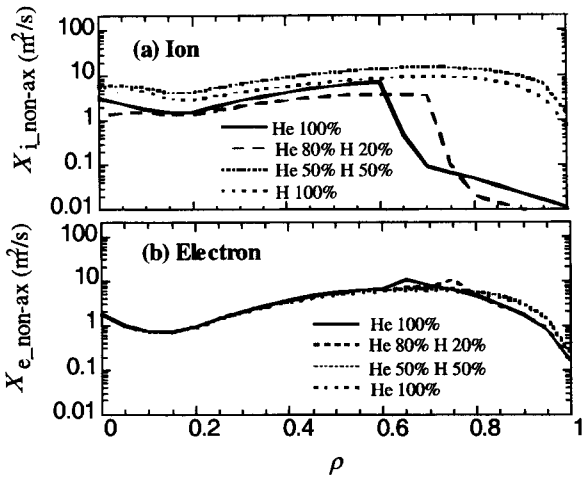

Fig. 5 (a) The profile of the ion thermal conductivity and (b) the profile of the electron thermal conductivity.

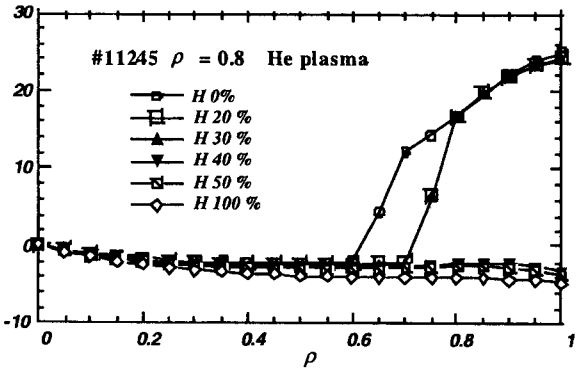

Fig. 6 The profile of the neoclassical E_r.

antenna to estimate the temperature in the long pulse discharge. We summarize the preceding argument as follows,

1. In the NBI (H ions were injected into He plasma) long pulse discharge of LHD, the decrement of the neoclassical conductivity of ions is observed in the periphery.
2. The above picture is significantly sensitive to the amount of H. It is predicted that the H injection in He discharge produces significant effect on the electric field and the polarity changes on the threshold of H quantity.

Acknowledgment

We would like to thank the members of LHD experimental group 1 and group 2 in National Institute for Fusion Science, for their work in maintaining and

operating LHD.

References

[1] S. Kubo *et al.*, Fusion Eng. Des. **26**, 319 (1995).

[2] Y. Nagayama *et al.*, Rev. Sci. Instrum. **70**, 1021 (1999).

[3] K.C. Shaing, Phys. Fluids **27**, 1567 (1984).

[4] K. Ida and S. Hidekuma, Rev. Sci. Instrum. **60**, 867 (1989).

[5] K. Kawahata, A. Ejiri, K. Tanaka, Y. Ito and S. Okajima, Fusion Eng. Des. **34-35**, 393 (1997).